JOURNAL OF SOLID STATE CHEMISTRY **137,** 289–294 (1998)
ARTICLE NO. SC977738

A Peroxoniobium Phosphate Derived from $NbOPO_4 \cdot 3H_2O$

Laureano Moreno-Real,* Enrique R. Losilla,* Miguel A. G. Aranda,* María Martínez-Lara,* Sebastián Bruque,* and Mercedes Gabás†

*Departamento de Química Inorgánica, Cristalografía y Mineralogía, Universidad de Málaga, 29071-Málaga, Spain; and
†Departamento de Física Aplicada, Universidad de Málaga, 29071 Málaga, Spain

Received July 30, 1997; in revised form December 18, 1997; accepted December 24, 1997

The reaction between white $NbOPO_4 \cdot 3H_2O$ and H_2O_2 produces yellow $NbO(O_2)_{0.5}PO_4 \cdot 2H_2O$. This reaction can be considered as an intercalation process since the Nb|P ratio and the basic layered structure are preserved. The X-ray powder diffraction pattern of the new phosphate can be indexed on a tetragonal unit cell with $a=6.488(1)$ Å and $c=16.030(4)$ Å. X-ray powder thermodiffractometry, DTA–TGA, Raman and IR spectroscopies, and magnetization measurements are used to characterize the new compound. The intercalated dioxygen bonds directly to niobium, replacing the water. Half of the initial NbO_6 groups change to NbO_7 since dioxygen acts a chelated ligand interacting with Nb through the two oxygens simultaneously. © 1998 Academic Press

INTRODUCTION

$NbOPO_4 \cdot 3H_2O$ (NbP) has a tetragonal layered structure similar to that of $VOPO_4 \cdot 2H_2O$ (1). The layers are formed by distorted NbO_6 octahedra and regular PO_4 tetrahedra. The four equatorial Nb–O bonds are roughly parallel to the layers making the infinite Nb–O–P linkage of the layers. There are two different axial Nb–O bonds: one short, which is characteristic of the niobyl group, and a long bond to the oxygen of the water molecule (Fig. 1). The detailed crystal structure of this compound is not known, as there is a strong disorder between layers leading to a poor crystalline material with broad X-ray powder diffraction peaks. The variable water content (the degree of hydration may vary between 2 and 3 water molecules per unit formula) and its consequences in the powder pattern also make niobyl phosphate trihydrate difficult to study by powder diffraction.

The nature of the water in the interlayer space of NbP has been studied by ^{1}H MAS NMR and IR techniques. Three water molecule types were observed in the spectroscopic studies and the positions and interactions were described (2). Upon intercalation, the sheets are spread apart, and several types of polar molecules may be taken up between the layers. For example, the intercalation of *n*-alkylamines, amides, alcohols, and other nitrogenous substances has been reported (3, 4). NbP can also intercalate phosphoric and sulfuric acids (3, 5).

In this study we describe the reaction between NbP and H_2O_2. The resulting peroxoniobium phosphate has been characterized by X-ray powder thermodiffractometry, thermal analysis, IR, Raman, and UV–vis spectroscopies, and magnetization measurements.

EXPERIMENTAL

Synthesis

$NbOPO_4 \cdot 3H_2O$ was synthesized as previously described (2). One gram of $NbOPO_4 \cdot 3H_2O$ was placed in contact with a mixture of isobutyl alcohol (50 ml) and H_2O_2 (3 ml, 30% w/w in water) at 60°C for 3 hr. The resulting yellow suspension was filtered, washed with cold bidistilled water, and dried at 40°C. Under these conditions, a single phase of $NbO(O_2)_{0.5}PO_4 \cdot 2H_2O$ (NboxoP) is obtained.

Characterization

The Nb/P ratio of NboxoP was determined by AEM using a Philips CM 200 Supertwin-DX4 with an Edax electron probe microanalyzer (Si–Li detector). The detector system has an ultrathin window, resulting in a resolution of 149 eV. Samples for the electron microscopy study were prepared as follows: a small amount was ground in an agate mortar and dispersed in absolute ethanol, and several drops of the resultant suspension were deposited onto a carbon-coated Formvar film supported on a copper grid. NbP was used as a standard for the AEM study.

Dioxygen content was determined by iodometric titration. Dioxygen and water contents were also determined by thermogravimetric analysis (TGA). Thermal analysis (DTA and TGA) was carried out in air on a Rigaku Thermoflex 8110 and Thermal Station TAS 100 apparatus at a heating rate of $10\,K\,min^{-1}$ with calcinated Al_2O_3 as standard reference.

0022-4596/98 $25.00

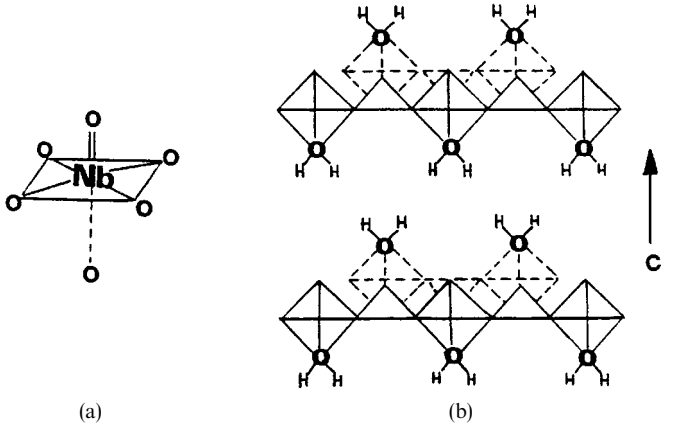

FIG. 1. (a) Six-coordinated geometry of niobiums in $NbOPO_4 \cdot 3H_2O$. (b) Layered structure viewed along the c axis of $NbOPO_4 \cdot 3H_2O$.

The room temperature powder diffraction pattern was collected on a Siemens D-501 automated diffractometer using graphite-monochromated Cu$K\alpha$ radiation. The powder thermodiffractometric study was carried out on a Siemens D-5000 diffractometer equipped with an HTK10 heating chamber. The patterns were scanned over the angular range 8–38° (2θ), with a step size of 0.04° and a scan rate of 1 s per step. The appropriate heating and cooling temperatures were selected by using the Diffract AT software. A delay time of 10 min was used before any pattern was acquired to ensure the transformations take place.

IR spectra were recorded on a Perkin-Elmer 883 spectrometer in the spectral range 4000–400 cm^{-1} using KBr pellets. Raman spectra were recorded on a Jobin Yvon Ramanor U1000 spectrometer using 514.5-nm excitation radiation generated by a Spectra Physics argon ion laser working at 300–500 mW. To increase the signal to noise ratio, a minimum of 10 scans were accumulated, resulting in a resolution of 2 cm^{-1}. The diffuse reflectance, UV–vis spectra were obtained on a Shimadzu UV-3100 spectrophotometer using an integrating sphere and $BaSO_4$ as the reference blank.

Magnetization measurements were performed on a Quantum Design MPMS-5 SQUID magnetometer. Data were collected in the 100–300 K temperature range using an applied magnetic field of 1000 Oe.

RESULTS AND DISCUSSION

Synthesis and Structural Characterization

The reaction between $NbOPO_4 \cdot 3H_2O$ and H_2O_2 in isobutyl alcohol yields $NbO(O_2)_{0.5}PO_4 \cdot 2H_2O$. The mechanism proposed for this reaction can be considered in two stages: (i) decomposition of H_2O_2, giving dioxygen; (ii) dioxygen diffusion in the interlayer space of the layered phosphate followed by (iii) dioxygen coordination to niobium with elimination of H_2O (Scheme 1). Several synthetic attempts to increase the dioxygen content were carried out by modifying the H_2O_2 concentration and by using several solvents. However, it has not been possible to increase the O_2 content of the sample. The final selected reaction medium was isobutyl alcohol instead of water to avoid hydrolysis, which decreases the reaction yield.

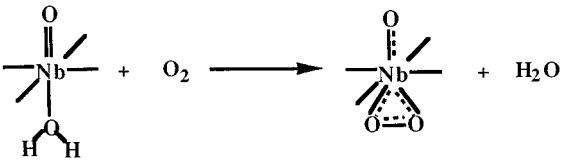

SCHEME 1. Reaction of dioxygen with $NbOPO_4 \cdot 3H_2O$ showing the initial and final niobium environments.

The chemical composition of the yellow phosphate is $NbO(O_2)_{0.5}PO_4 \cdot 2H_2O$, which maintains the Nb/P ratio of the starting compound. The X-ray powder diffraction pattern of NboxoP was autoindexed by using the TREOR90 program (6) on a tetragonal unit cell with $a =$ 6.488(1) Å and $c = 16.030(4)$ Å with a figure of merit $M(20) = 21$ (7) and $F(20) = 25$ (0.017, 47) (8). These parameters show that the layered structure of the pristine solid is maintained. NbP and NboxoP have the same type of tetragonal layers as anhydrous α-$NbOPO_4$ with $a = 6.387$ Å. However, the ordering along the c axis is modified to accommodate the dioxygen molecule between the layers. Since the Nb/P ratio and the layers are preserved, this preparative reaction can be considered to be an intercalation process.

$VOPO_4 \cdot 2H_2O$ crystallizes on a tetragonal structure: space group $P4/nmm$, $a = 6.202$ Å, $c = 7.410$ Å, $V = 285.0$ $Å^3$, $Z = 2$, V_{at} (per non-hydrogen atom) = 15.8 $Å^3$/atom (1). $NbO(O_2)_{0.5}PO_4 \cdot 2H_2O$ also crystallizes on a tetragonal structure: $a = 6.488$ Å, $c = 16.029$ Å, $V = 674.7$ $Å^3$, $Z = 4$, $V_{at} = 16.8$ $Å^3$/atom. The observed systematic absences are compatible with the $P4_2/n$ space group. Attempts to refine the structure in the new cell using an adapted $VOPO_4 \cdot 2H_2O$ type structure as a starting model were unsuccessful. *Ab initio* structure determination methodology was also tried without success. This is probably due to the strong preferred orientation effect and to the broad peaks due to small microparticle sizes and microstrains induced in the intercalation reaction. A related cell has been reported for $NaMoO(HPO_4)_{0.5}PO_4 \cdot H_2O$ from single-crystal data: space group $I4/mmm$, $a = 6.452$ Å, $c = 15.999$ Å, $V = 666.0$ $Å^3$, $Z = 4$, $V_{at} = 14.5$ $Å^3$/atom (9). However, this structure is body centered and the systematic absences in $NbO(O_2)_{0.5}PO_4 \cdot 2H_2O$ unambiguously indicated a primitive cell. The difference in the structures of all these materials is the stacking order of the layers along the c axis direction, the individual layers being very similar. The ligand that is bonded to the metal in the layers is H_2O in the pristine

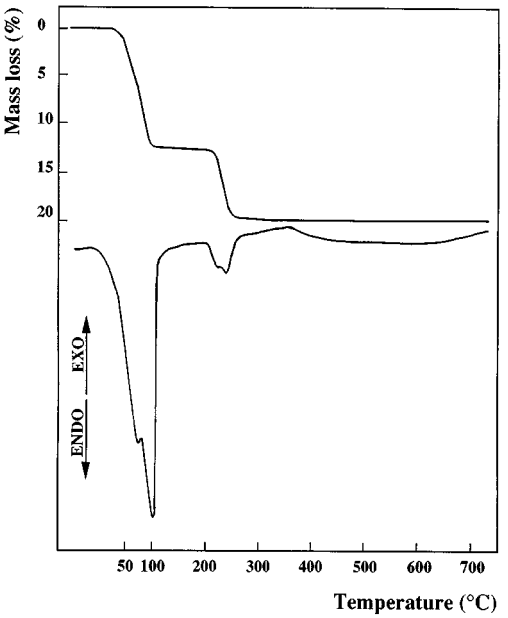

FIG. 2. TGA–DTA curves for $NbO(O_2)_{0.5}PO_4 \cdot 2H_2O$.

materials but it also may be HPO_4^{2-}, O_2, or others in the solids obtained by intercalation reactions.

Thermal and Thermodiffractometric Study

The TGA and DTA curves of NboxoP are shown in Fig 2. There are two different stages in the thermal decomposition of this compound. First, there are two intense endotherms at 75 and 100°C due to the loss of two water molecules. The observed mass loss, 12.5%, agrees with that calculated for the loss of two water molecules, 14.0%. Second, the release of dioxygen groups is evident as two small endotherms centered at 235 and at 250°C (observed mass loss, 7.3%; calculated for the release of dioxygen, 6.3%). This last step was also monitored by mass spectrometry to determine the gas evolved. It was confirmed that at these temperatures ($\approx$240°C) dioxygen was released. Thus, only dioxygen molecules are present in the interlayer space above 130°C. The interaction between dioxygen and niobium has to be strong as this coordination compound is stable up to $\approx$230°C.

It is worth emphasizing that the stoichiometry of NboxoP is fixed, resulting in a single interlayer *d* spacing at 8.0 Å. The variable water content in NbP results in several diffraction peaks between 7.5 and 8 Å. X-ray powder thermodiffractometric data for NboxoP (Fig. 3) and NbP (Fig. 4) were collected to determine the layered structure stability with temperature. For both layered phosphates, the final thermal decomposition product is anhydrous α-$NbOPO_4$, which has a 3D structure originating from layer collapsing (10). The peak at $\approx 27.5°$ (2θ), 3.2 Å, corresponds to the (200) reflection and so it is independent of the layer arrangement along the *c* axis. This peak is clearly visible in both room temperature patterns and, furthermore, it does not change on heating when α-$NbOPO_4$ is obtained. The interlayer space of the peroxoniobium phosphate is preserved up to 220°C whereas the layers for NbP start to collapse above 100°C, which shows the higher thermal stability of the peroxoniobium phosphate.

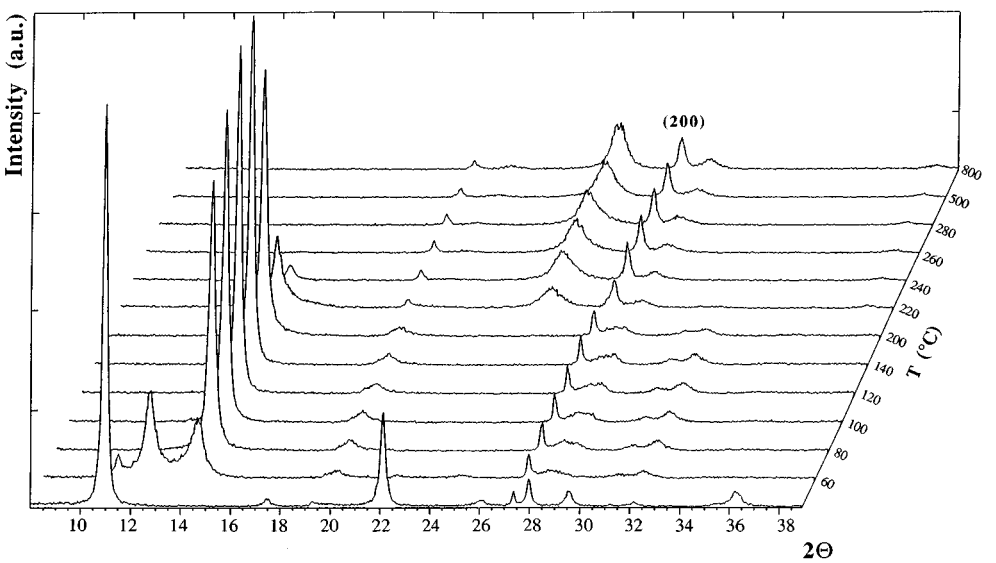

FIG. 3. X-ray thermodiffractometric powder patterns for $NbO(O_2)_{0.5}PO_4 \cdot 2H_2O$.

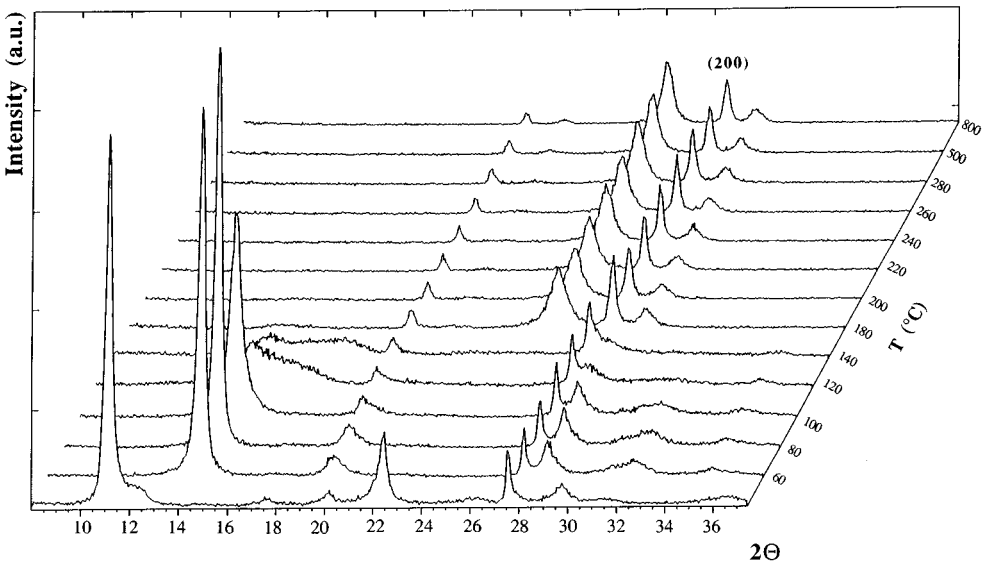

FIG. 4. X-ray thermodiffractometric powder patterns for $NbOPO_4 \cdot 3H_2O$.

IR and Raman Studies

Figures 5a and 5b show the IR spectra of NboxoP and NbP, respectively. There are differences in the region between 600 and 500 cm^{-1}, with NboxoP showing two new bands at 605 and 525 cm^{-1}. The O–O stretching vibration (ν_2) at $\approx 880\ cm^{-1}$ and, more importantly, the bending mode around 1400 cm^{-1} (ν_3) of H_2O_2 in the liquid and frozen states do not appear (11). This indicates that the ligand is not H_2O_2. The Raman spectra of NboxoP and NbP are shown in Figs. 6a and 6b, respectively. Three new bands are detected in the Raman spectrum of NboxoP, centered at 915, 604, and 540 cm^{-1} for ν(O–O) (ν_1) and ν(Nb–O_2) (ν_2 and ν_3), respectively. From the Raman spectra, a chelated geometry (C_{2v}) for dioxygen coordination to niobium can be suggested, since this symmetry implies three vibration modes which are active in both IR and Raman spectra. These assignments are based on comparisons with other dioxygen–metal complexes (12–15). An end-on Nb–O–O bonding type can be discarded as this symmetry should give a higher O–O stretching vibration in the 1030- to 1180-cm^{-1} region (12).

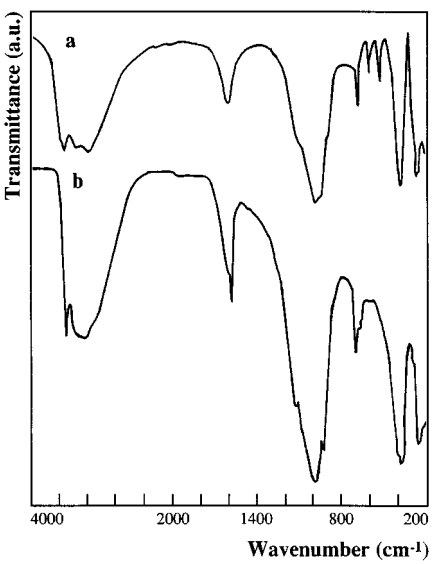

FIG. 5. IR spectra for (a) $NbO(O_2)_{0.5}PO_4 \cdot 2H_2O$ and (b) $NbOPO_4 \cdot 3H_2O$.

The comparative study of the vibrational spectra is adequate as a full analysis of the vibrations based on the symmetry of the unit cell (factor group) is not possible. The average symmetry determined from the X-ray powder study is tetragonal C_{4h}^4, but the local symmetry of the unit cell is unknown (orthorhombic or lower) due to the coordination of the O_2 groups to the niobiums located at the initial fourfold axis. The long-range disorder of these groups leads to the average observed tetragonal symmetry.

The band due to the Nb=O stretching vibration at 950 cm^{-1} for NbP noticeably decreases in intensity and is shifted to 936 cm^{-1} for NboxoP. This change cannot be detected in the infrared spectra since the Nb=O stretching frequency is masked by PO_4 vibrations. The spectral change is a consequence of the two different niobium environments. Half of the niobiums are still linked to one water molecule, as in the pristine phosphate, showing six-coordinated geometry, and ν(Nb=O) is located at 936 cm^{-1} instead of 950 cm^{-1}. This slight displacement is due to some structural modifications that occur during the dioxygen intercalation

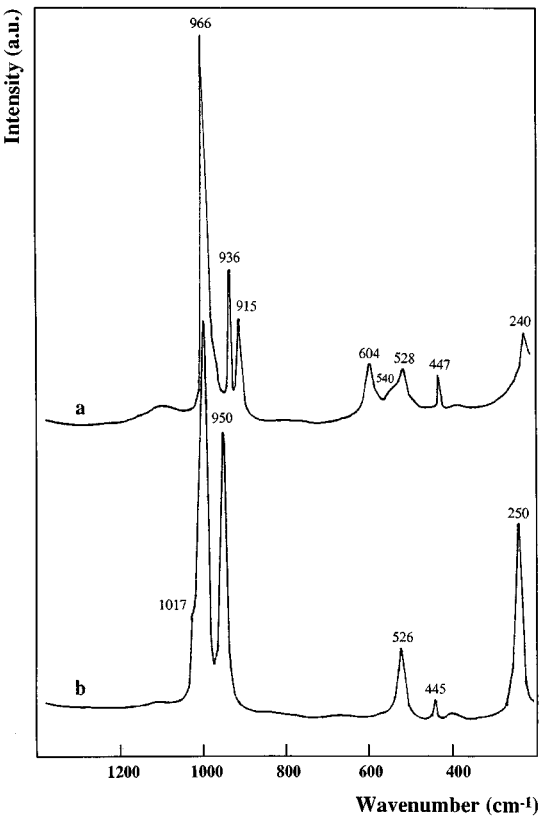

FIG. 6. Raman spectra for (a) $NbO(O_2)_{0.5}PO_4 \cdot 2H_2O$ and (b) $NbOPO_4 \cdot 3H_2O$.

process: changes in the NbO_6 site symmetry or Nb–O bonding (16). The band at 936 cm^{-1} has a lower intensity than the band at 950 cm^{-1} because it is only related to half of the niobiums. The remaining niobium atoms cannot exhibit this vibration because they have seven coordinated geometry. In the NbO_7 geometry, there are four oxygens in the equatorial plane and three in apical positions. These three oxygens can generate an electron relaxation system (see Scheme 1) with important influences on the nature of the Nb–O and O–O bands: the Nb=O double bond disappears and the lengths of the three axial Nb–O bonds and the O–O bond are affected.

This relaxation in the O–O bond is evidenced by the O–O stretching vibration at 915 cm^{-1}, which corresponds to a peroxo-like group rather than a Nb–O–O superoxo configuration. All transition metal complexes with a cyclic peroxide configuration and equimolecular metal–dioxygen ratio have ν(O–O) between 800 and 930 cm^{-1} (12). The bands between 995 and 1017 cm^{-1} for both phosphates involve the stretching vibrations of the PO_4 tetrahedra. On the other hand, bands below 525 cm^{-1} can be assigned to O–P–O and O–Nb–O bending vibrations, with a high degree of coupling (17). The band around 250 cm^{-1} can be assigned mainly to the O–Nb–O bending mode since the intensity of this band decreases notably for peroxoniobium phosphate. From vibrational data it is possible to suggest a strong interaction of dioxygen with niobium after the intercalation process.

Diffuse Reflectance Spectroscopy Study

Figures 7a and 7b show the UV–vis spectra of NboxoP and NbP, respectively. NbP presents a unique strong absorption band at 235 nm whereas NboxoP exhibits two intense bands at 240 and 344 nm. All these bands are due to charge-transfer processes (L → M type), which are expected for transition metals with a high oxidation state and a d^0 electronic configuration (18). It can be deduced that the charge-transfer peak at 344 nm is responsible for the yellow color of NboxoP.

Magnetization Study

The magnetization curves for NboxoP and NbP are shown in Figs. 8a and 8b, respectively. The magnitude of the magnetic response of both samples was extremely weak and a high applied magnetic field, 1000 Oe, was necessary to obtain measurable signals. NbP shows a diamagnetic behavior around room temperature, typical of a Nb^{5+} cation with a d^0 electronic configuration. Below $\approx$250 K, the

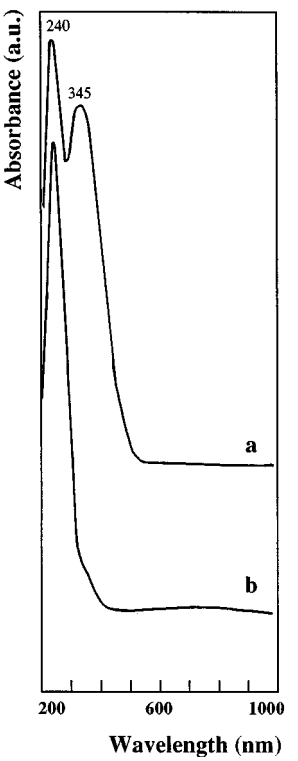

FIG. 7. UV–vis spectra for (a) $NbO(O_2)_{0.5}PO_4 \cdot 2H_2O$ and (b) $NbOPO_4 \cdot 3H_2O$.

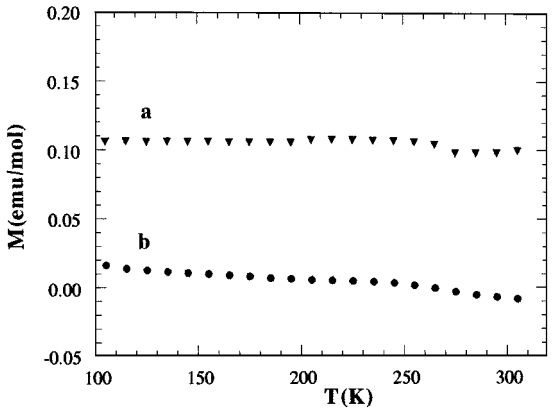

FIG. 8. Magnetization curves for (a) $NbO(O_2)_{0.5}PO_4 \cdot 2H_2O$ and (b) $NbOPO_4 \cdot 3H_2O$ under a 1000 Oe applied magnetic field.

signal becomes positive, probably due to the presence of a very small amount of impurity.

NboxoP shows a clear temperature-independent paramagnetism (TIP) behavior in the measured temperature range. Niobium atoms linked to O_2 present a heptacoordination of oxygens with a highly distorted environment. In such low-symmetry environments, as detected in the vibrational study, TIP behavior is usually related to polarization paramagnetism, also know as Van Vleck paramagnetism (19). Since NboxoP is obtained from NbP, both samples should contain the same impurity. As already discussed, at $\approx$250 K there is a change in the magnetisation sign of NbP. At the same temperature, there is a small step in the magnetization curve for NboxoP. These two variations are probably due to the same impurity.

The intercalation of dioxygen generates a solid, NboxoP, which has a more distorted local structure with NbO_7 groups. This new environment, which does not exist in NbP, is responsible for the different observed magnetic behavior. TIP has also been observed in related systems such as chromates and permanganates with diamagnetic transition metals in high oxidation states (20). These compounds display strong charge-transfer bands such as that observed in the diffuse reflectance study of NboxoP.

Finally, it is expected that NboxoP could be used in some catalytic systems since there are some oxidation reactions in which species susceptible to oxidation do not react directly with free molecular O_2.

CONCLUSIONS

A new niobyl phosphate, $NbO(O_2)_{0.5}PO_4 \cdot 2H_2O$, has been synthesized by intercalation of dioxygen into $NbOPO_4 \cdot 3H_2O$. The layers are similar in these two phosphates and in the thermal decomposition product, α-$NbOPO_4$, as shown by thermodiffractometry study. The thermal stability of $NbO(O_2)_{0.5}PO_4 \cdot 2H_2O$ is higher than that of $NbOPO_4 \cdot 3H_2O$ since the layers start to collapse above 230 and 120°C, respectively. Dioxygen bonds to the axial position of the niobium, increasing the coordination number from six to seven as dioxygen acts as a chelating ligand. The chelated niobium–dioxygen geometry has been determined by vibrational spectroscopy. Magnetization measurements have shown a TIP behavior for the intercalated material.

ACKNOWLEDGMENTS

This work was supported by CICYT research grant PB 93/1245 from the Ministerio de Educación y Ciencia, Spain, and the research grant team FQM-113 of the Junta de Andalucía, Spain. We thank Dr. Conrado Rillo (ICMA, CSIC-Univ. Zaragoza) for his help with the magnetization measurements.

REFERENCES

1. H. R. Tietze, *Aust. J. Chem.* **34,** 2035 (1981).
2. S. Bruque-Gámez, M. Martínez-Lara, L. Moreno-Real, A. Jiménez-López, B. Casal, and E. Ruiz-Hitzky, *Inorg. Chem.* **26,** 847 (1987).
3. K. Beneke and G. Lagaly, *Inorg. Chem.* **22,** 1503 (1983).
4. A. García-Ponce, L. Moreno-Real, and A. Jiménez-López, *Can. J. Chem.* **68,** 592 (1990).
5. N. G. Chernorukov, N. P. Egonov, and I. A. Korshunov, *Izv. Akad. Nauk SSSR, Neorg. Mater.* **15,** 335 (1979).
6. P. E. Werner, L. Eriksson, and M. Westdahl, *J. Appl. Crystallogr.* **18,** 367 (1985).
7. P. M. Wolff, *J. Appl. Crystallogr.* **1,** 108 (1968).
8. G. S. Smith and R. L. Snyder, *J. Appl. Crystallogr.* **12,** 60 (1979).
9. R. Peascoe and A. Clearfield, *J. Solid State Chem.* **95,** 289 (1991).
10. J. M. Longo and P. Kierkegaard, *Acta Chem. Scand.* **20,** 72 (1966).
11. K. Nakamoto, "Infrared Spectra of Inorganic and Coordination Compounds," 2nd ed. Wiley-Interscience, London, 1970.
12. L.Vaska, *Acc. Chem. Res.* **9,** 175 (1976).
13. R. D. Jones, D. A. Summerville, and F. Basolo, *Chem. Rev.* **79,** 139 (1979).
14. M. N. Bhattacharjee, M. K. Chaudhuri, and N. S. Islam, *Inorg. Chem.* **28,** 2420 (1989).
15. S. Ahmad, J. D. McCallum, A. K. Shiemke, E. H. Appelman, T. M. Loehr, and J. Sanders-Loehr, *Inorg. Chem.* **27,** 2230 (1988).
16. G. T. Stranford and R. A. Condrate, *J. Solid State Chem.* **76,** 407 (1988).
17. G. T. Stranford and R. A. Condrate, *J. Solid State Chem.* **52,** 248 (1984).
18. A. B. P. Lever, "Inorganic Electronic Spectroscopy," 2nd ed. (Elsevier Science Publishers, Amsterdam, 1984.
19. J. H. Van Vleck, *Phys. Rev.* **31,** 587 (1928).
20. R. L. Carlin, "Magnetochemistry." Springer-Verlag, Berlin, 1986.